Effect of oxygen content on the magnetic properties of multiferroic $YMn_2O_{5+\delta}$

2009 J. Phys.: Condens. Matter 21 346002

(http://iopscience.iop.org/0953-8984/21/34/346002)

J. Phys.: Condens. Matter **21** (2009) 346002 (5pp) doi:10.1088/0953-8984/21/34/346002

Effect of oxygen content on the magnetic properties of multiferroic $YMn_2O_{5+\delta}$

C Ma[1,2], J-Q Yan[1], K W Dennis[1], A Llobet[3], R W McCallum[1,2] and X Tan[1,2]

[1] Division of Materials Science and Engineering, Ames Laboratory, US-DOE, Ames, IA 50011, USA
[2] Department of Materials Science and Engineering, Iowa State University, Ames, IA 50011, USA
[3] Los Alamos Neutron Science Center, Lujan Neutron Scattering Center, Los Alamos National Laboratory, Los Alamos, NM 87545, USA

E-mail: xtan@iastate.edu

Received 10 April 2009, in final form 5 June 2009
Published 28 July 2009
Online at stacks.iop.org/JPhysCM/21/346002

Abstract
The effect of oxygen content on magnetic properties in the multiferroic $YMn_2O_{5+\delta}$ system was investigated with samples prepared under different oxygen pressures. Our results show that, with increasing oxygen content, the magnetic response changes from being dominated by the anomaly at ∼45 K to the one around 20 K. However, specific heat measurements and neutron powder diffraction studies indicate that the presence of the magnetic transition at ∼45 K is independent of oxygen content. The results suggest that oxygen nonstoichiometry can be one important degree of freedom in manipulating the multiferroic properties.

(Some figures in this article are in colour only in the electronic version)

1. Introduction

Multiferroic materials have been studied extensively over the years due to their interesting magnetic and dielectric properties and their mutual coupling [1–4]. YMn_2O_5 is one of the very few compounds which display multiferroism [5–7]. The YMn_2O_5 compound crystallizes in an orthorhombic structure with the space group *Pbam*. The unit cell contains two crystallographic sites for Mn cations, with different oxygen coordinations and oxidation states: the Mn^{4+} ion is located at the 4f site and is octahedrally coordinated to oxygen, whereas Mn^{3+} occupies the 4h site and is bonded to five oxygen atoms, forming a distorted pyramid [8]. The crystal structure contains infinite chains of edge-sharing Mn^{4+} O_6 octahedra, running along the *c* axis (in *Pbam* notation) and the different chains are interconnected by the Mn^{3+} O_5 pyramids and RO_8 scalenohedra.

YMn_2O_5 displays four magnetic phase transitions at low temperatures [5–7]. With decreasing temperature, YMn_2O_5 orders as 2D and 1D incommensurate magnetic structures at 45 K and 40 K, respectively. Below 39 K the magnetic order becomes commensurate with the propagation vector $\mathbf{q} = (\frac{1}{2}, 0, \frac{1}{4})$. On further cooling below 20 K, the magnetic structure orders as a low temperature incommensurate (LT-ICM) one. Two ferroelectric phase transitions were observed at 39 K and 20 K, respectively [5, 9]. At 39 K, the spontaneous polarization develops along the *b* axis, accompanied by a sharp peak in the dielectric permittivity when measured along this axis, while at 20 K, the dielectric permittivity shows a step-like anomaly [5, 9]. Both these ferroelectric transitions occur right at the magnetic transition temperatures. It is believed that the ferroelectric order is induced by the magnetic order [10–12]. Therefore, the investigation of the magnetic phase transitions is critical in understanding the multiferroic mechanism in YMn_2O_5 and other RMn_2O_5 compounds (R = Y, Bi and rare earth).

Oxygen nonstoichiometry plays an important role in controlling the peculiar physical properties of transition metal oxides [13, 14]. This is expected to be true for the RMn_2O_5 oxide family since Mn has both 3+ and 4+ valence states in the compound. Alonso *et al* noticed that RMn_2O_5 (R = La, Pr, Nd, Sm and Eu) prepared under 200 bar oxygen atmosphere were off-stoichiometry and oxygen-rich [15]. Chen *et al* reported that the oxygen content in $LaMn_2O_5$ can be varied from 5.01 to 5.17 using a hydrothermal synthesis process [16]. However, how magnetic properties are affected by oxygen

nonstoichiometry in RMn_2O_5, including YMn_2O_5, has not yet been systematically studied. In the present work, we synthesized $YMn_2O_{5+\delta}$ with different oxygen contents and observed a ferromagnetic component below 20 K in samples with high oxygen content, which has not been reported in YMn_2O_5 previously.

2. Experimental procedure

Single-phase $YMn_2O_{5+\delta}$ was prepared by a modified Pechini's method as described elsewhere [17]. Oxygen content was varied by calcining the precursor pellets at 1000 °C under 1, 2.5, 5 and 10 bar of oxygen pressure for 30 h, respectively. The samples were then furnace-cooled to room temperature in the same atmosphere. The phase purity of all samples was verified by x-ray powder diffraction with monochromatic Cu Kα radiation. The oxygen content was determined using iodometric titration, assuming the molar ratio of Y:Mn = 1:2 [18]. The magnetic characterization was performed with a Superconducting Quantum Interference Device (Quantum Design). The temperature dependence of specific heat was measured in the temperature range from 1.8 to 300 K with a physical property measurement system (Quantum Design). Neutron powder diffraction was performed at the High Intensity Powder Diffractometer (HIPD), Los Alamos Neutron Science Center, Los Alamos National Laboratories.

3. Results and discussion

The oxygen content determined with iodometric titration for samples calcined under 1, 2.5, 5 and 10 bar oxygen pressure is 4.98, 4.99, 5.02 and 5.07, respectively. X-ray diffraction patterns at room temperature confirmed that all samples are single phase and the patterns could be indexed with the *Pbam* space group. Rietveld refinement of the room temperature x-ray diffraction pattern revealed that the lattice parameters, within the limit of uncertainty, agree with previous results [17, 19] and seem not to vary with oxygen content.

In an effort to resolve the delicate structural difference between those samples with various oxygen contents, neutron powder diffraction measurements were performed from 15 to 300 K. Structural refinements were carried out using the General Structure Analysis System (GSAS) program [20], in which isotropic thermal parameters (*Uiso*) of Y and Mn and anisotropic thermal parameters (*Uaniso*) for oxygen were used. The final average R factor is $Rwp = 3.5\%$ with an average $\chi^2 \sim 1.6$. Table 1 lists the room temperature data of lattice parameters, selected bond lengths and angles for $YMn_2O_{4.98}$ and $YMn_2O_{5.07}$. The lattice parameters for both samples are the same within the resolution limit. From the data of bond distances and angles, it is found that the $Mn1O_5$ tetragonal pyramids are almost identical in these two compositions except that the two Mn1–O1 bond distances are slightly shortened with increasing oxygen content. A noticeable difference was observed for the $Mn2O_6$ octahedron and Mn2–O–Mn2 bond angles, as highlighted with the bold font in table 1. When the oxygen content increases from 4.98 to 5.07, the $Mn2O_6$ octahedron is contracted along the O4–Mn2–O4 direction.

Table 1. Lattice parameters a, b and c (Å), selected bond distances (Å) and angles (degree) for $YMn_2O_{4.98}$ and $YMn_2O_{5.07}$ at room temperature. Noticeable changes are highlighted in bold. Mn1 refers to Mn^{3+} at 4 h (x, y, 1/2); Mn2 refers to Mn^{4+} at 4f (0, 1/2, z); O1, O2, O3 and O4 are the O^{2-} ion at 4e (0, 0, z), 4g (x, y, 0), 4 h (x, y, 1/2) and 8i (x, y, z), respectively.

	$YMn_2O_{4.98}$	$YMn_2O_{5.07}$
a	7.26278(9)	7.26258(10)
b	8.46992(9)	8.47051(10)
c	5.66599(6)	5.66531(6)
Mn1–O1(×2)	1.9257(13)	1.9210(15)
Mn1–O3(×1)	2.0182(15)	2.0182(17)
Mn1–O4(×2)	1.8966(12)	1.8982(14)
⟨Mn1–O⟩	1.9326	1.9313
Mn2–O2(×2)	***1.9240(12)***	***1.9286(14)***
Mn2–O3(×2)	***1.8667(12)***	***1.8629(14)***
Mn2-O4(×2)	***1.9085(6)***	***1.9064(7)***
⟨Mn2–O⟩	1.8997	1.8993
Mn1–O1–Mn1	95.12(7)	95.11(8)
Mn2–O2–Mn2	***97.27(7)***	***97.45(8)***
Mn2–O3–Mn2	***96.17(8)***	***95.89(9)***
Mn1–O4–Mn2	122.30(6)	122.35(7)

Despite the slight changes in the crystal structure, dramatic changes in the temperature dependence of magnetization were observed in $YMn_2O_{5+\delta}$ with different oxygen content. Figure 1 shows magnetization M versus temperature T curves for $YMn_2O_{5+\delta}$ samples taken with $H = 100$ Oe in a field-cooling (FC) mode. With decreasing temperature, magnetization of $YMn_2O_{4.98}$ shows a sharp increase at $T \sim 45$ K and then saturates at low temperatures (figure 1(a)). No anomaly was observed at the CM–ICM transition around ∼20 K. The transition temperature and temperature dependence of magnetization are consistent with previous reports [10]. In sharp contrast to the $YMn_2O_{4.98}$ sample, the temperature dependence of magnetization in $YMn_2O_{5.07}$ is dominated by an increase in the vicinity of 20 K when temperature is decreased (figure 1(c)). The magnetization increase at ∼20 K is an order of magnitude greater than that observed in $YMn_2O_{4.98}$ at ∼45 K. A slope change in the $1/M(T)$ curve is barely observed at $T \sim 45$ K in $YMn_2O_{5.07}$. The $M(T)$ curve of $YMn_2O_{4.99}$, displays two anomalies at $T \sim 20$ K and ∼45 K, respectively, although the transitions become broader (figure 1(b)).

Figure 2 shows the magnetization M versus field H curves for both $YMn_2O_{4.98}$ and $YMn_2O_{5.07}$. At 35 K, both samples show a linear relation between M and H. At 5 K, the linear relation between M and H persists for $YMn_2O_{4.98}$. The M versus H curve for $YMn_2O_{5.07}$ displays a slope change at $H = \pm 3$ kOe, suggesting the existence of a ferromagnetic component. A small hysteresis of magnetization at low fields was also observed. At 5 K, the ferromagnetic moment obtained from extrapolating the high field linear part to $H = 0$ Oe is 9.46×10^{-3} μ_B/Mn.

In order to verify the barely observable anomaly at ∼45 K in $YMn_2O_{5.07}$ is intrinsic, specific heat (C_p) of $YMn_2O_{4.98}$ and $YMn_2O_{5.07}$ samples was measured and compared with that of a single crystal grown with the flux method under flowing oxygen. Figure 3(a) displays the results measured in the heating direction. The single crystal displays all the transitions reported in previous studies [19]: two lambda anomalies at

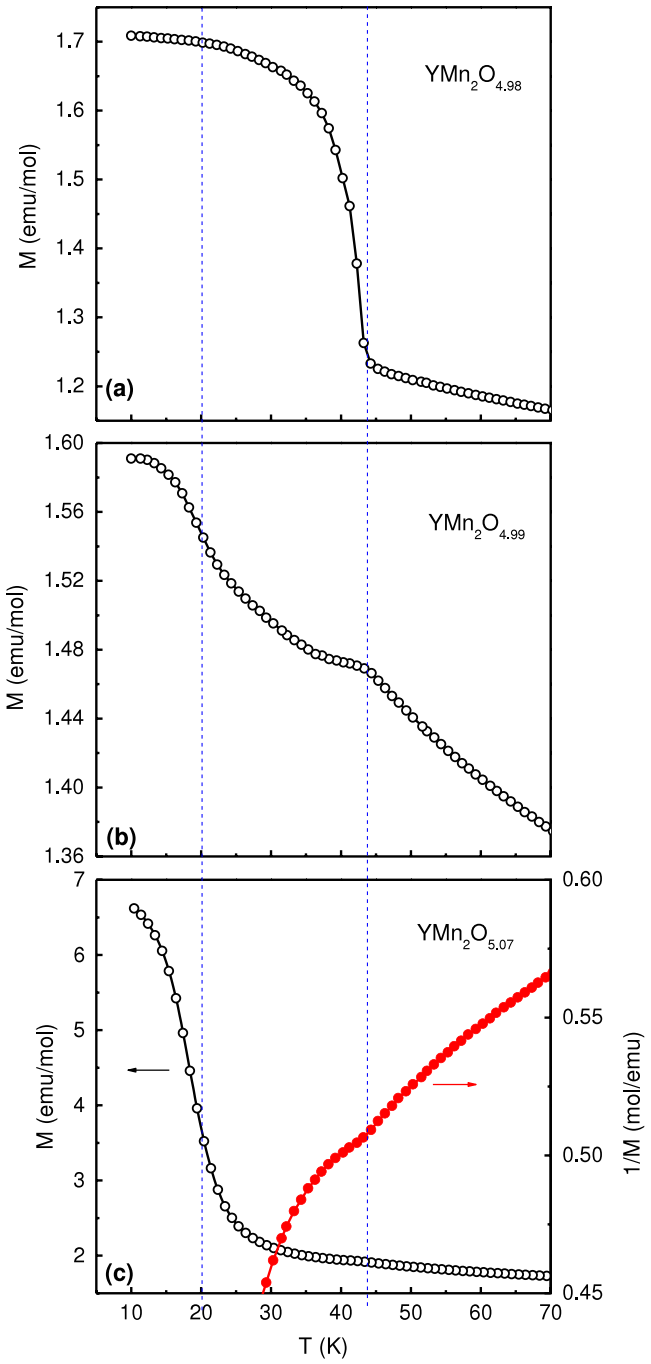

Figure 1. Temperature dependence of magnetization of (a) $YMn_2O_{4.98}$, (b) $YMn_2O_{4.99}$ and (c) $YMn_2O_{5.07}$ measured under a magnetic field of 100 Oe with the field-cooling mode. The temperature dependence of the inverse magnetization of $YMn_2O_{5.07}$ is also plotted in (c) to reveal the weak anomaly at ∼45 K. The vertical dotted lines indicate the two transitions at ∼45 K and ∼20 K, respectively.

∼44 K and ∼40 K, respectively, and a thermal hysteresis around 20 K (the cooling-down measurement is not shown here). In contrast, C_p of $YMn_2O_{4.98}$ and $YMn_2O_{5.07}$ shows only one broad lambda anomaly at ∼45 K. The broadening may be due to the polycrystalline nature of the samples. No other anomaly could be well resolved below 40 K. The magnitude of the entropy change at ∼45 K is roughly the same

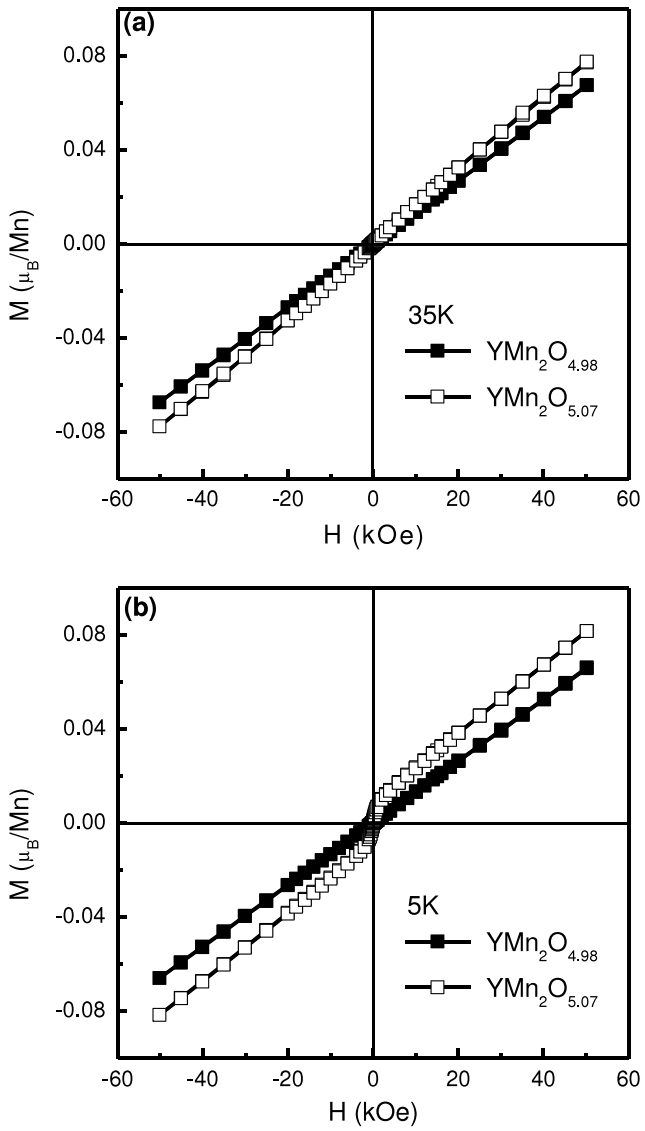

Figure 2. The magnetization M versus magnetic field H curves of the $YMn_2O_{4.98}$ and the $YMn_2O_{5.07}$ samples measured at (a) 35 K and (b) 5 K.

for both $YMn_2O_{4.98}$ and $YMn_2O_{5.07}$, which suggests that the anomaly around ∼45 K in $YMn_2O_{5.07}$ is intrinsic, not from a possible minor impurity phase.

Further support comes from the neutron powder diffraction experiment in the temperature range of 15 K $\leqslant T \leqslant$ 300 K. Figure 3(b) shows the temperature dependence of the intensity of the $(0, 1, 0) \pm \mathbf{q}$ magnetic reflection for both $YMn_2O_{4.98}$ and $YMn_2O_{5.07}$ samples. It was found that both samples displayed a magnetic ordering at $T < 45$ K and there is no distinguishable difference in the magnetic reflections between the two samples. The almost identical diffraction patterns suggest no significant change of the magnetic structure with oxygen content up to 5.07.

The ferromagnetism found in $YMn_2O_{5.07}$ below 20 K is not from a possible minor impurity phase either. Y^{3+} cations carry no magnetic moment; possible magnetic impurities are Mn–O binaries, $YMnO_3$ and $Y_2Mn_2O_7$. Of these

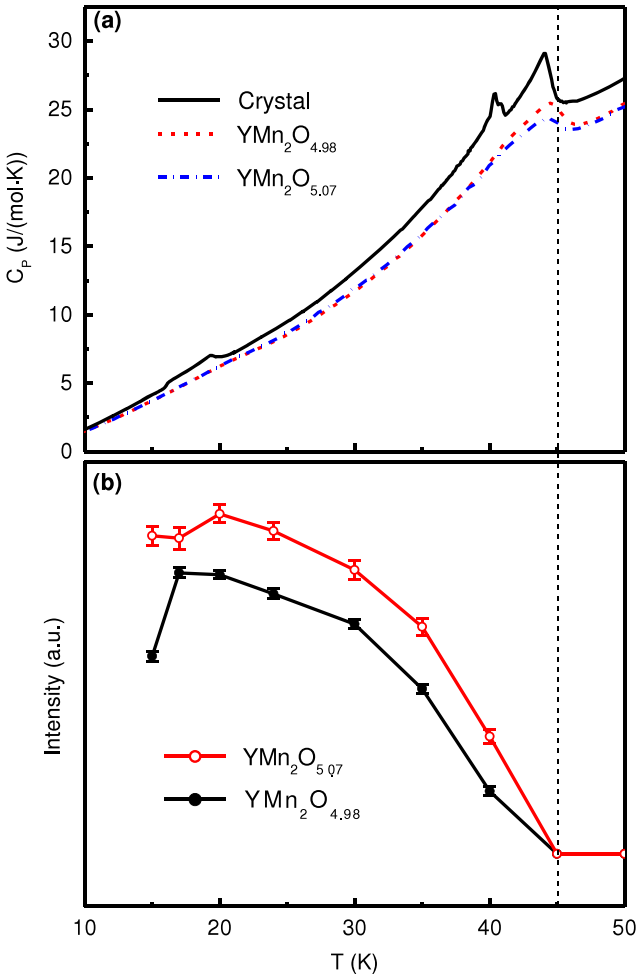

Figure 3. (a) Temperature dependence of specific heat C_p for a single crystal of YMn_2O_5, polycrystalline $YMn_2O_{4.98}$ and $YMn_2O_{5.07}$ measured in the heating direction. (b) Temperature dependence of the intensity of the (0, 1, 0) $\pm$ **q** magnetic reflection for $YMn_2O_{4.98}$ and $YMn_2O_{5.07}$.

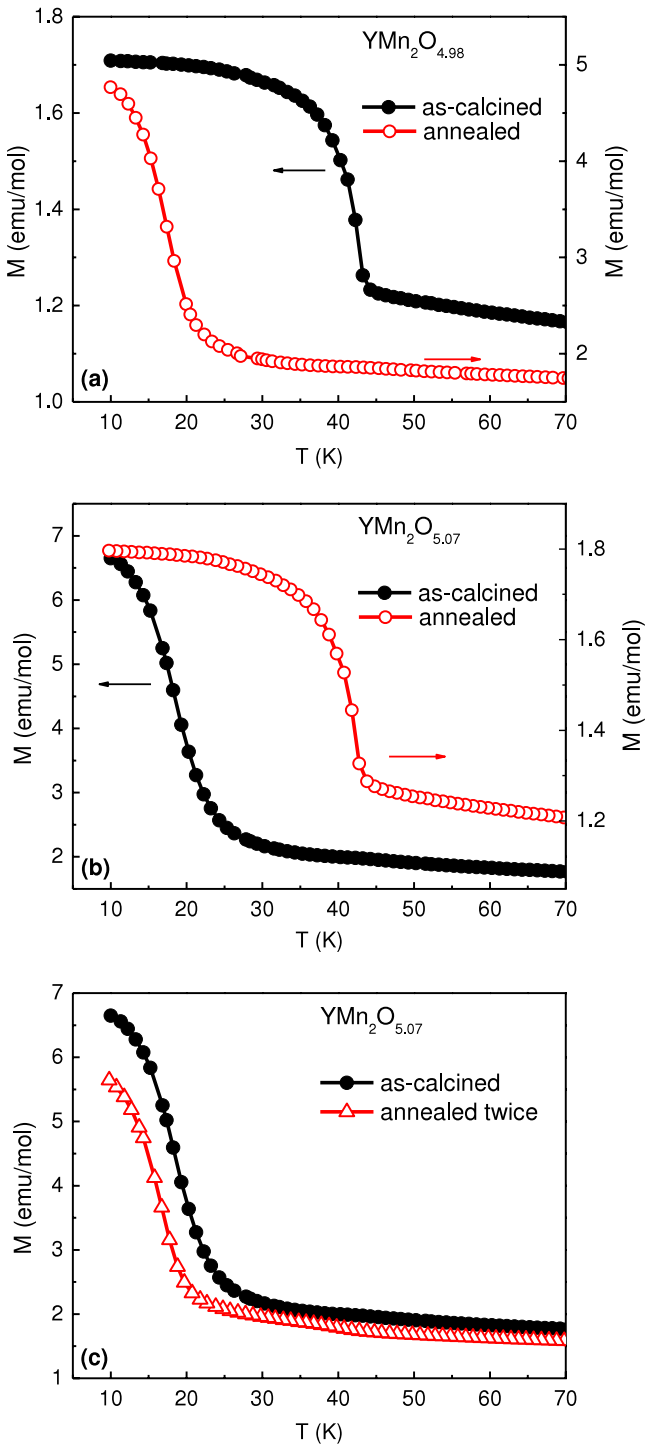

Figure 4. Effect of post-process annealing on the temperature dependence of magnetization measured under 100 Oe with the field-cooling procedure. (a) As-calcined $YMn_2O_{4.98}$ and after annealing at 1000 °C in 10 bar O_2 for 18 h, (b) as-calcined $YMn_2O_{5.07}$ and after annealing at 1020 °C in air for 18 h, (c) as-calcined $YMn_2O_{5.07}$ and after two successive anneals: (i) 1020 °C in air for 18 h and then (ii) 1000 °C in 10 bar O_2 for 30 h.

compounds, only $Y_2Mn_2O_7$ displays a magnetic transition around 20 K [21–23]. However, the formation of $Y_2Mn_2O_7$ at 1000 °C requires an oxygen pressure of 40–60 kbar and a standard thermogravimetric test in air indicated a decomposition temperature of 800 °C [21, 22]. The $YMn_2O_{5.07}$ sample in the present study was prepared at 1000 °C under 10 bar oxygen pressure and furthermore, as will be shown later in the post-process annealing experiments, it is thermally stable in air to temperatures above 1000 °C.

Thus the excess oxygen does not significantly change the magnetic order at ~45 K, but introduces a very small ferromagnetic component below the transition at ~20 K in $YMn_2O_{5+\delta}$. The neutron powder diffraction study at low temperatures does not reveal any observable difference between the magnetic structures, including the incommensurability parameters, in $YMn_2O_{4.98}$ and $YMn_2O_{5.07}$. The linear M–H relation of $YMn_2O_{4.98}$ and $YMn_2O_{5.07}$ at 35 K and that of $YMn_2O_{4.98}$ at 5 K is consistent with that of a compensated antiferromagnet. The nonlinear M–H relation and the ferromagnetic component for $YMn_2O_{5.07}$ at 5 K suggests that the uncompensated magnetic moment is most likely due to spin canting. The change of spin orientation due to oxygen nonstoichiometry will affect the net polarization in the incommensurate magnetic phase below 20 K [11]. Thus oxygen nonstoichiometry can be employed to manipulate not only the magnetic properties, but also the fer-

roelectric properties in RMn_2O_5. The dielectric measurement of these $YMn_2O_{5+\delta}$ samples with different oxygen contents is currently underway and will be reported later. Moreover, the enhanced magnetic moment in oxygen-rich samples is expected to lead to an enhanced effect of a magnetic field on the ferroelectric properties at low temperatures.

The oxygen content in the as-calcined $YMn_2O_{5+\delta}$ samples can be reversibly altered by post-process annealing, resulting in reversibly altered magnetic behaviors. Figure 4 displays the change in the temperature dependence of magnetization under $H = 100$ Oe after annealing in the $YMn_2O_{4.98}$ and $YMn_2O_{5.07}$ samples. The temperature dependence of magnetization of $YMn_2O_{4.98}$ becomes similar to that of $YMn_2O_{5.07}$ after annealing at 1000 °C in 10 bar O_2 for 18 h where the anomaly at ∼45 K almost disappears (figure 4(a)). This indicates that oxygen in the atmosphere has been incorporated into the sample and oxygen-rich samples result after the annealing. However, removing the excess oxygen from the as-calcined $YMn_2O_{5.07}$ turns out to be a little harder. A higher temperature and a lower oxygen partial pressure are needed compared to the calcination conditions. Figure 4(b) shows the temperature dependence of magnetization of the $YMn_2O_{5.07}$ sample after annealing in air at 1020 °C for 18 h. The post-process annealing makes the weak transition at ∼45 K dominant, as in the as-calcined $YMn_2O_{4.98}$ sample. In addition, the magnitude of the magnetization in the annealed sample is almost identical to that in the as-calcined $YMn_2O_{4.98}$ sample. Furthermore, after the annealed $YMn_2O_{5.07}$ sample (1020 °C, 18 h, air) was annealed one more time at 1000 °C under 10 bar oxygen pressure for 30 h, the original magnetic behavior in the as-calcined $YMn_2O_{5.07}$ sample was recovered, as demonstrated in figure 4(c).

4. Conclusions

In summary, we studied the effect of oxygen nonstoichiometry in multiferroic $YMn_2O_{5+\delta}$. Excess oxygen is found to introduce a ferromagnetic component in the low temperature incommensurate magnetic phase. Oxygen content can be reversibly controlled by post-process annealing under different temperatures and atmospheres. Due to the intimate coupling between the magnetic and ferroelectric behaviors in the RMn_2O_5 oxide family, it is expected that oxygen nonstoichiometry can be used to tune the ferroelectric properties as well. Such studies are currently underway.

Acknowledgments

Ames Laboratory is operated for the US Department of Energy by Iowa State University under contract no. DE-AC02-07CH11358. The neutron diffraction work was performed at the Lujan Center at Los Alamos Neutron Science Center. Los Alamos National Laboratory is operated by Los Alamos National Security LLC under DOE contract DE-AC52-06NA25396.

References

[1] Kimura T, Goto T, Shintani H, Ishizaka K, Arima T and Tokura Y 2003 *Nature* **426** 55
[2] Hui N, Park S, Sharma P, Ahn J, Guha S and Cheong S W 2004 *Nature* **429** 392
[3] Wang J, Neaton J B, Zheng H, Nagarajan V, Ogale S B, Liu B, Viehland D, Vaithyanathan V, Schlom D G, Waghmare U V, Spaldin N A, Rabe K M, Wuttig M and Ramesh R 2003 *Science* **299** 1719
[4] Fiebig M 2005 *J. Phys. D: Appl. Phys.* **38** R123
[5] Kobayashi S, Osawa T, Kimura H, Noda Y, Kagomiya I and Kohn K 2004 *Japan. J. Phys. Soc.* **73** 1593
[6] Noda Y, Kimura H, Kamada Y, Ishikawa Y, Kobayashi S, Wakabayashi Y, Sawa H, Ikeda N and Kohn K 2007 *J. Korean Phys. Soc.* **51** 828
[7] Radaelli P G and Chapon L C 2008 *J. Phys.: Condens. Matter* **20** 434213
[8] Alonso J A, Casais M T, Martínez-Lope M J, Martínez J L and Fernández-Díaz M T 1997 *J. Phys.: Condens. Matter* **9** 8515
[9] Kohn K 1994 *Ferroelectrics* **162** 1
[10] Kadomtseva A M, Popov Y F, Vorobev G P, Kamilov K I, Makhov P N, Tehranchi M M and Phirouznia A 2003 *Physica* B **329** 856
[11] Chapon L C, Radaelli P G, Blake G R, Park S and Cheong S W 2006 *Phys. Rev. Lett.* **96** 097601
[12] Noda Y, Kimura H, Kamada Y and Osawa T 2006 *Physica* B **385** 119
[13] Töpfer J and Goodenough J B 1997 *J. Solid State Chem.* **130** 117
[14] Suard E, Maignan A, Caignaert V and Raveau B 1992 *Physica* C **200** 43
[15] Alonso J A, Casais M T, Martínez-Lope M J and Rasines I 1997 *J. Solid State Chem.* **129** 105
[16] Chen Y, Yuan H, Tian G, Zhang G and Feng S 2007 *J. Solid State Chem.* **180** 1340
[17] Ma C, Yan J-Q, Dennis K W, McCallum R W and Tan X 2009 *J. Appl. Phys.* **105** 033908
[18] Licci F, Turilli G and Ferro P 1996 *J. Magn. Magn. Mater.* **164** L268
[19] Tachibana M, Akiyama K, Kawaji H and Atake T 2005 *Phys. Rev.* B **72** 224425
[20] Larson A and von Dreele R B 1994 General structure analysis system (GSAS) *Los Alamos National Laboratory Report* LAUR 86-748
[21] Fujinaka H, Kinamura N, Koizumi M, Miyamoto Y and Kume S 1979 *Mater. Res. Bull.* **14** 1133
[22] Subramanian M A, Torardi C C, Johnson D C, Pannetier J and Sleight A W 1988 *J. Solid State Chem.* **72** 24
[23] Reimers J N, Greedan J E, Kremer R K, Gmelin E and Subramanian M A 1991 *Phys. Rev.* B **43** 3387